XLVI CILAMCE
VITÓRIA - ES - BRAZIL - 2025
XLVI IBERO-LATIN AMERICAN CONGRESS ON COMPUTATIONAL METHODS IN ENGINEERING

A Novel Kinematics-Based Approach for Fiber-Reinforced Sandwich Beams Considering Continuous Shear Stress Response

Thyago Andrade Mota[1], Fabio Carlos da Rocha[1]

[1]*Dept. of Civil Engineering, Federal University of Sergipe*
Av. Marcelo Deda Chagas, 49107-230, São Cristóvão-SE, Brazil
thyagoandrade@academico.ufs.br, fabiocrocha@academico.ufs.br

Abstract. Sandwich beams are widely used in engineering because of their high stiffness-to-mass ratio and manufacturing efficiency. However, their mechanical response features zigzag longitudinal displacement and interlaminar shear that classical beam theories cannot accurately capture. This study introduces a refined higher-order zigzag theory that enforces shear stress continuity across layer interfaces, thereby overcoming the limitations of classical beam theories. Governing equations are derived from Lagrange's principle and solved via the Rayleigh–Ritz method. Validation against Pagano's elasticity solution for a simply-supported cross-ply beam under sinusoidal loading shows excellent agreement: Weighted Absolute Percentage Error (WAPE) of 0.36% (deflection), 3.34% (longitudinal displacement), 0.73% (shear stress), and 1.37% (normal stress). These results demonstrate improved accuracy in capturing the mechanical response of laminated composite beams.

Keywords: Sandwich beams; Zigzag theory; Higher-order beam model; Shear stress continuity; Fiber reinforced composite.

1 Introduction

According to Reddy [1], composite materials are formed by combining different materials on a macroscopic scale and consist of two main phases: the matrix and the reinforcement. According to Jones [2], the matrix represents the continuous phase of the material, being responsible for protecting the reinforcements and transmitting external loads between them. In turn, the reinforcement corresponds to the discontinuous phase and may consist of fibers, flakes, or particles. According to Kaw [3], these materials have several advantages, such as high mechanical and thermal resistance, high rigidity, corrosion resistance, and good thermal conductivity, which justifies their wide application in different areas of engineering.

This work aims to fill a gap in the literature related to the static analysis of bending in laminated composite beams by considering the continuity of interlaminar shear stress, incorporated by a new kinematic formulation. Unlike existing RZT approaches, the present formulation defines zigzag and amplitude functions to enforce displacement and stress compatibility across interfaces, ensuring continuous interlaminar shear without additional equilibrium constraints. The equations of motion are derived from Lagrange's principle and solved numerically using cross-ply, simply supported, and subjected to sinusoidal loading, with the results compared to those obtained by Pagano [4], based on elasticity theory

2 Mathematical Development

2.1 Kinematics

Some mathematical notation is necessary for the development of the formulation. The following symbols are used for the derivative of functions $\hat{A}_{,\triangleleft} := \partial\hat{A}/\partial\triangleleft$ and $\hat{A}_{,\triangleleft\bigcirc} := \partial^2\hat{A}/\partial\triangleleft\partial\bigcirc$. When matrix notation is used, the symbol $[\hat{A}]$ represents a matrix or matrix row, and $\{\hat{A}\}$ is associated with a column of a matrix.

Consider a domain beam $\Omega \subset \mathbb{R}^3$, referenced to the Cartesian axes $x-y-z$, as shown in Fig. 1. The displacement field for the analysis of the sandwich beam is expressed according to eq. (1).

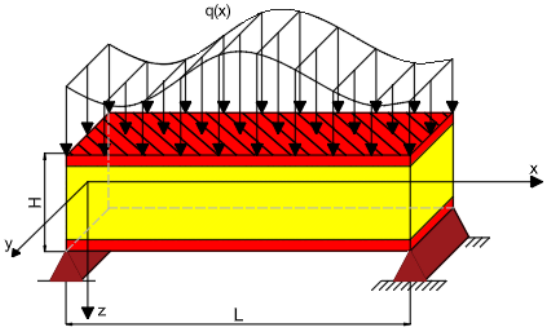


Figure 1. Sandwich beam subjected to sinusoidal loading

$$u_x^{(k)}(x,z) = u_o(x) + zq_x + y_x(x)f_x^{(k)}(z) + x_x^{(k)}(x)(a^{(k)}(z))^2 + h_x^{(k)}(x)(a^{(k)}(z))^3,\ u_z(x,z) = w(x), \tag{1}$$

where $u_x^{(k)}(x,z)$ and $u_z(x,z)$ represent, respectively, the displacements in the directions x and z. The index $k=1,\ 2,\ 3$ indicates the numbering of the layer and the displacement in the direction y is disregarded. The variables $u_o(x)$, z, θ_x, $\psi_x(x)$, and $f_x^{(k)}(z)$ correspond, respectively, to the axial displacement on the mean axis, the elevation about the mean axis, the total rotation of the cross-section about the axis y, the amplitude function and the zigzag function of the RZT model proposed by Tessler et al. [5]. In addition, $\xi_x^{(k)}(x)$ and $\eta_x^{(k)}(x)$ are unknown functions that guarantee the compatibility of displacement and stress between the layers. The function $\alpha^{(k)}(z)$ refers to the local coordinate system of the k-th layer, as shown in eq. (2).

$$\alpha^{(k)}(z) = z - \frac{(z^{(k-1)} + z^{(k)})}{2},\ z^{(k)} \le z \le z^{(k-1)}. \tag{2}$$

Considering elastic-linear material and using eq. (1) it is possible to express the strain and stress fields as shown in eqs. (3) and (4).

$$\varepsilon_x^{(k)}(x,z) = u_{o,x}(x) + z\theta_{x,x} + \psi_{x,x}(x)\phi_x^k(z) + \xi_{x,x}^{(k)}(x)(\alpha^{(k)}(z))^2 + \eta_{x,x}^{(k)}(x)(\alpha^{(k)}(z))^3,\ 2\varepsilon_{xz}^{(k)}(x,z) = u_{x,z}^{(k)} + u_{z,x}, \tag{3}$$

$$\sigma_x^{(k)}(x,z) = C_{11}^{**(k)}(z)\varepsilon_x^k(x,z),\ \tau_{xz}^{(k)}(x,z) = C_{55}^{**(k)}(z)\left(2\varepsilon_{xz}^{(k)}(x,z)\right), \tag{4}$$

where $C_{11}^{**(k)}(z)$ and $C_{55}^{**(k)}(z)$ are the material properties of each layer k, given by

$$C_{11}^{**(k)}(z) = \bar{C}_{11}^{(k)}(z) - \bar{C}_{13}^{(k)}(z)\ \bar{C}_{13}^{(k)}(z)/\bar{C}_{33}^{(k)}(z),\ C_{55}^{**(k)}(z) = \bar{C}_{55}^{(k)}(z) - \bar{C}_{45}^{(k)}(z)\ \bar{C}_{45}^{(k)}(z)/\bar{C}_{44}^{(k)}(z), \tag{5}$$

with $\bar{C}_{11}^{(k)}(z) = C_{11}(z)\ \mathrm{Cos}^4\varphi + 2\left(C_{12}(z) + 2C_{66}(z)\right)\ \mathrm{Cos}^2\varphi\ \mathrm{Sin}^2\varphi + C_{22}(z)\ \mathrm{Sin}^4\varphi$, $\bar{C}_{13}^{(k)}(z) = C_{13}(z)\ \mathrm{Cos}^2\varphi + C_{23}(z)\ \mathrm{Sin}^2\varphi$, $\bar{C}_{33}^{(k)}(z) = C_{33}(z)$, , $\bar{C}_{55}^{(k)}(z) = C_{55}(z)\ \mathrm{Cos}^2\varphi + C_{44}(z)\ \mathrm{Sin}^2\varphi$, $\bar{C}_{44}^{(k)}(z) = C_{44}(z)\ \mathrm{Cos}^2\varphi + C_{55}(z)\ \mathrm{Sin}^2\varphi$ and $\bar{C}_{45}^{(k)}(z) = \left(-C_{44}(z) + C_{55}(z)\right)\ \mathrm{Cos}\varphi\ \mathrm{Sin}\varphi$. The terms $C_{ij}(z)$, with $i,\ j \in \{1,\ldots,6\}$, are the coefficients of stiffness for an orthotropic material obtained in Reddy[1] and φ is the angle of rotation of the fiber about the axis z.

Imposing the conditions of compatibility between layers for the response fields, and nullity of the shear stress at the upper and lower edges of the beam, according to eq. (6), the functions $\xi_x^{(k)}(x)$ and $\eta_x^{(k)}(x)$ as shown in eq. (7).

$$\sigma_{xz}^{(1)}(x,z_o) = \sigma_{xz}^{(N)}(x,z_N) = 0,\ \sigma_{xz}^{(k-1)}(x,z_k) = \sigma_{xz}^{(k)}(x,z_k),\ u_{xz}^{(k-1)}(x,z_k) = u_{xz}^{(k)}(x,z_k), \tag{6}$$

$$\xi_x^{(k)}(x) = a_1^k\left(\theta_y(x) + u_z(x,z)\right) + b_1^k\ \psi_x(x),\ \eta_x^{(k)}(x) = a_2^k\left(\theta_y(x) + u_z(x,z)\right) + b_2^k\ \psi_x(x), \tag{7}$$

where $a_1^{(k)}$, $a_2^{(k)}$, $b_1^{(k)}$ and $b_2^{(k)}$ are real constants that depend on the layer.

Replacing the eq. (7) in eqs. (1), (3), and (4), and the displacement and stress fields are rewritten in matrix notation according to eq. (8).

$$u_x^{(k)}(x,z)=\left[T_1^{(k)}(z)\right]\left\{d_1(x)\right\}+\left[T_2^{(k)}(z)\right]\left\{d_{1,x}(x)\right\},\ u_z^{(k)}(x,z)=\left[T_3\right]\left\{d_1(x)\right\}, \tag{8}$$

$$\varepsilon_x^{(k)}(x,z)=\left[T_1^{(k)}(z)\right]\left\{d_{1,x}(x)\right\}+\left[T_2^{(k)}(z)\right]\left\{d_{1,xx}(x)\right\},\ 2\varepsilon_{xz}^{(k)}(x,z)=\left[T_{1,z}^{(k)}(z)\right]\left\{d_1(x)\right\}+\left[T_4^{(k)}(z)\right]\left\{d_{1,x}(x)\right\}, \tag{9}$$

$$\sigma_x^{(k)}(x,z)=\left[T_5^{(k)}(z)\right]\left\{d_{1,x}(x)\right\}+\left[T_6^{(k)}(z)\right]\left\{d_{1,xx}(x)\right\},\ \tau_{xz}^{(k)}(x,z)=\left[T_7^{(k)}(z)\right]\left\{d_1(x)\right\}+\left[T_8^{(k)}(z)\right]\left\{d_{1,x}(x)\right\}. \tag{10}$$

Where $\left\{d_1(x)\right\}=\left[u_o(x)\quad\theta(x)\quad\psi(x)\quad w(x)\right]^T$, $\left[T_1^{(k)}(z)\right]=\left[1\quad z+P_x^{(k)}(z)\quad\phi_x^{(k)}(z)+Q_x^{(k)}(z)\quad 0\right]$, $\left[T_2^{(k)}(z)\right]=\left[0\quad 0\quad 0\quad P_x^{(k)}(z)\right]$, $\left[T_3^{(k)}(z)\right]=\left[0\quad 0\quad 0\quad 1\right]$, $\left[T_4^{(k)}(z)\right]=\left[T_{1,z}^{(k)}(z)\right]+\left[T_3\right]$, $\left[T_5^{(k)}(z)\right]=C_{11}^{**(k)}(z)\left[T_1^{(k)}(z)\right]$, $\left[T_6^{(k)}(z)\right]=C_{11}^{**(k)}(z)\left[T_2^{(k)}(z)\right]$, $\left[T_7^{(k)}(z)\right]=C_{55}^{**(k)}(z)\left[T_{1,z}^{(k)}(z)\right]$, $\left[T_8^{(k)}(z)\right]=C_{55}^{**(k)}(z)\left[T_4^{(k)}(z)\right]$.

2.2 Energy functional

For a solid occupying a region $\Omega\subset\mathbb{R}^3$, of volume v, the total energy is given by (Reddy[6]):

$$\prod(U,V)=U+V, \tag{11}$$

where U and V represent the internal deformation energy and the potential energy, respectively, for a linear elastic orthotropic material, subjected to an external force $q_z(x)$ at the top and bottom edges, is given by the eq. (12) and (13) (Reddy [6]).

$$U\left(\varepsilon_x,\varepsilon_{xz},\sigma_x,\sigma_{xz}\right)=\frac{1}{2}\int_v\left[\left\{\varepsilon_x^{(k)}(x,z)\right\}^T\sigma_x^{(k)}(x,z)+\left\{2\varepsilon_{xz}^{(k)}(x,z)\right\}^T\sigma_{xz}^{(k)}(x,z)\right]dv. \tag{12}$$

$$V\left(u_z,q_z\right)=-\int_0^L\left[u_z^{(k)}\left(x,z^*\right)\right]^T q_z(x)dx. \tag{13}$$

where z^* is the quota on the top $\left(z^*=-h/2\right)$ or lower $\left(z^*=h/2\right)$ edge of the laminate.

2.3 Solution by Rayleigh- Ritz method

In the Rayleigh-Ritz method, the response fields are approximated by polynomial series with N terms, according to eq. (14), and consisting of unknowns $\left(u_m,\ \theta_m,\ \psi_m,\ w_m\right)$ and approximate functions $\left(K_m^u(x),\ K_m^\theta(x)\right.$, $\left.K_m^\psi(x)\ \ K_m^w(x)\right)$, which satisfy the interest boundary conditions.

$$u_o(x)=\sum_{m=1}^N K_m^u(x)\cdot u_m,\ \theta(x)=\sum_{m=1}^N K_m^\theta(x)\cdot\theta_m,\ \psi(x)=\sum_{m=1}^N K_m^\psi(x)\cdot\psi_m,\ w(x)=\sum_{m=1}^N K_m^w(x)\cdot w_m, \tag{14}$$

The approximation functions used in this study were those developed by Nguyen *et al.* [7] and presented here in eq. (15).

$$K_m^u(x)=K_m^\theta(x)=K_m^\psi(x)=C_j^*\left(\frac{x}{L}\right)C_j^*\left(\frac{x}{L}-1\right),\ K_m^w(x)=\left[C_j^*\left(\frac{x}{L}\right)C_j^*\left(\frac{x}{L}-1\right)\right]_{,x}, \tag{15}$$

where $C_j^*(X)$ are functions defined as presented in eq. (16) and dependent on Chebychev polynomials of the first type, as per eq. (17).

$$C_j^*(X)=C_j(1-X)-1, \tag{16}$$

where C_j are the ChebyChev polynomials (type I) constructed by the recurrence formula presented in the eq. (17).

$$C_0(X)=1,\ C_1(X)=X,\ C_{j+1}(X)=2XC_j(X)-C_{j-1}(X), \tag{17}$$

where $X \in [0,1]$ and j =1, N .

The terms of eq. (14) are reorganized matricially, according to eq. (18). Next, eq. (18) is substituted into eq. (11) and Lagrange's principle is applied, as shown in eq. (19), to obtain the stationary system shown in eq. (20).

$$\{d_1(x)\}=\sum_{m=1}^{N}\begin{bmatrix} K_m^u(x) & 0 & 0 & 0 \\ 0 & K_m^\theta(x) & 0 & 0 \\ 0 & 0 & K_m^\psi(x) & 0 \\ 0 & 0 & 0 & K_m^w(x) \end{bmatrix}\begin{Bmatrix} u_m \\ \theta_m \\ \psi_m \\ w_m \end{Bmatrix}=\sum_{m=1}^{N}[K]_m\{d\}_m. \tag{18}$$

$$\begin{aligned} &\frac{\partial\Pi}{\partial u_m}=\frac{\partial U(u_m,\theta_m,\psi_m,w_m)}{\partial u_m}+\frac{\partial V(w_m)}{\partial u_m}=0,\ \frac{\partial\Pi}{\partial \theta_m}=\frac{\partial U(u_m,\theta_m,\psi_m,w_m)}{\partial \theta_m}+\frac{\partial V(w_m)}{\partial \theta_m}=0, \\ &\frac{\partial\Pi}{\partial \psi_m}=\frac{\partial U(u_m,\theta_m,\psi_m,w_m)}{\partial \psi_m}+\frac{\partial V(w_m)}{\partial \psi_m}=0,\ \frac{\partial\Pi}{\partial w_m}=\frac{\partial U(u_m,\theta_m,\psi_m,w_m)}{\partial w_m}+\frac{\partial V(w_m)}{\partial w_m}=0. \end{aligned} \tag{19}$$

$$\sum_{m=1}^{N}\left[\tilde{K}_z\right]_r^m\{d\}_m-\{F\}_r=0, \tag{20}$$

where the terms $\left[\tilde{K}_z\right]_r^m$ and $\{F\}_r$ are designated by the eqs. (21) and (22).

$$\left[\tilde{K}_z\right]_r^m=\int_0^L\begin{bmatrix}[K_{,x}]_r^T A_1[K_{,x}]_m+[K_{,x}]_r^T A_2[K_{,xx}]_m+[K_{,xx}]_r^T A_3[K_{,x}]_m+[K_{,xx}]_r^T A_4[K_{,xx}]_m+ \\ [K]_r^T A_5[K]_m+[K]_r^T A_6[K_{,x}]_m+[K_{,x}]_r^T A_7[K]_m+[K_{,x}]_r^T A_8[K_{,x}]_m\end{bmatrix}dx, \tag{21}$$

$$\{F\}_r=-\int_0^L\left([K(x_\square)]_r^T[T_3]^T q_z(x)\right)dx, \tag{22}$$

and

$$\begin{aligned} &A_1=\int_A\left[T_1^{(k)}(z)\right]^T\left[T_5^{(k)}(z)\right]dA,\ A_2=\int_A\left[T_1^{(k)}(z)\right]^T\left[T_6^{(k)}(z)\right]dA,\ A_3=\int_A\left[T_6^{(k)}(z)\right]^T\left[T_1^{(k)}(z)\right]dA, \\ &A_4=\int_A\left[T_2^{(k)}(z)\right]^T\left[T_6^{(k)}(z)\right]dA,\ A_5=\int_A\left[T_{1,z}^{(k)}(z)\right]^T\left[T_7^{(k)}(z)\right]dA,\ A_6=\int_A\left[T_{1,z}^{(k)}(z)\right]^T\left[T_8^{(k)}(z)\right]dA, \\ &A_7=\int_A\left[T_8^{(k)}(z)\right]^T\left[T_{1,z}^{(k)}(z)\right]dA,\ A_8=\int_A\left[T_4^{(k)}(z)\right]^T\left[T_8^{(k)}(z)\right]dA. \end{aligned} \tag{23}$$

2.4 Results and discussion

In order to verify the accuracy of the proposed formulation, the results obtained by the elasticity theory, as developed by Pagano [4], were adopted as a reference. For validation, the static flexural behavior of a laminated composite beam, simply supported, reinforced by fibers with 0°/90°/0° stacking and submitted to a sinusoidal loading, was analyzed. The analysis considers the elastic-linear regime and the plane state of stress. The properties of the materials, including the longitudinal and transverse modulus of elasticity, as well as the Poisson coefficients, are presented in Table 1. In addition, a beam with unit width (b) and height (h), and length (L) equal to five times your height

Table 1. Mechanical properties of the beam layers

Property	Symbol	Value (GPa)
Longitudinal Modulus of Elasticity	E_1	25.0
Longitudinal Modulus of Elasticity	$E_2 = E_3$	1.00
Transversal Modulus of Elasticity	$G_{12} = G_{13}$	0.20
Transversal Modulus of Elasticity	G_{23}	0.50

The stress and displacement fields were nondimensionalized according to eq. (24). To analyze the error in the response fields of interest along a cross section, the Weighted Absolute Percentage Error (WAPE) metric, defined in eq. (25) was employed.

$$\bar{\sigma}_x = \frac{\sigma_x\left(L/2,z\right)}{q_0}, \bar{\sigma}_{xz} = \frac{\sigma_{xz}\left(0,z\right)}{q_0}, \bar{u} = \frac{E_T^{(1)} \cdot u\left(0,z\right)}{h \cdot q_0}, \bar{w} = \frac{100 \cdot E_T^{(1)} \cdot h^3 \cdot w\left(x,0\right)}{q_0 \cdot L^4}, \bar{x} = \frac{x}{h}, \bar{z} = \frac{z}{h}. \tag{24}$$

$$WAPE = 100 \frac{\sum_{j=1}^{n} \left| x_j - X_j \right|}{\sum_{j=1}^{n} \left| X_j \right|}, \tag{25}$$

Here, $E_T^{(1)}$ denotes the longitudinal modulus of elasticity in the direction transverse to the fibers for the first layer, q_0 is the maximum value of the sinusoidal loading; and x_i and X_j represent, respectively, the reference values and those predicted by the proposed model.

Figure 2-a and Fig. 2-b illustrate the variation of the shear stress $\left(x=0\right)$ and normal stress $\left(x=L/2\right)$, respectively, along the height of the beam. In the case of shear stress (Fig. 2-a), its intensity increases towards the midline and vanishes at the edges. Conversely, for normal stress (Fig. 2-b), the intensity increases toward the outer surfaces and diminishes at the beam's mid-height.

Figure 2-a also highlights the continuity of the shear stress as predicted by the constitutive equation (eq. 10), without requiring the application of the equilibrium equation, as is typically done in previous studies. Similarly to shear stress, the normal stress exhibits excellent agreement between the reference results and the present model. This agreement is confirmed both qualitatively, via Figs. 2-a and 2-b, and quantitatively, by the WAPE metric, which yielded values of 0.73% for shear stress and 1.37% for normal stress.

Figure 3-a and Fig. 3-b present the deflection along the midline $\left(z=0\right)$ and the longitudinal displacement at $x=0$, respectively. As shown in Fig. 3-b, the proposed model successfully captures the zigzag effect predicted by elasticity theory (Pagano [4]). Both figures demonstrate excellent qualitative and quantitative agreement between the proposed model and the reference solution. Quantitatively, this is supported by the WAPE metric, which yielded error values of 0.36% for deflection and 3.34% for longitudinal displacement.

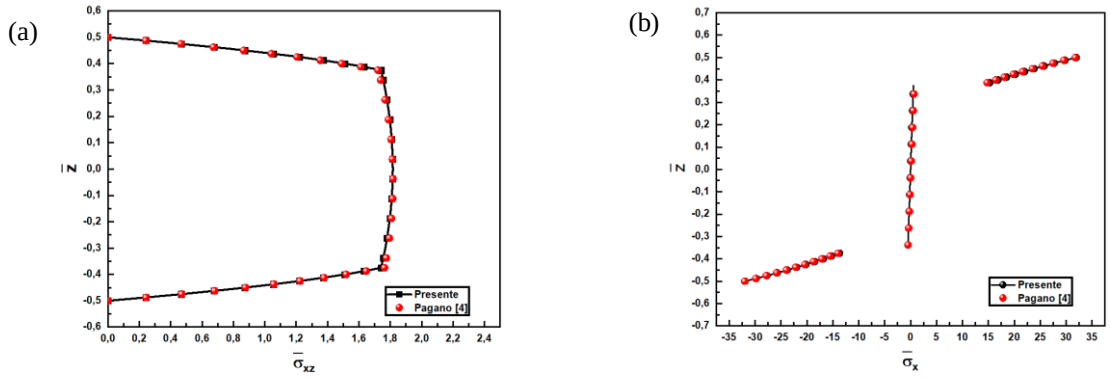


Figure 2. (a) shows the shear stress at $x=0$, and (b) shows the normal stress at $x=L/2$

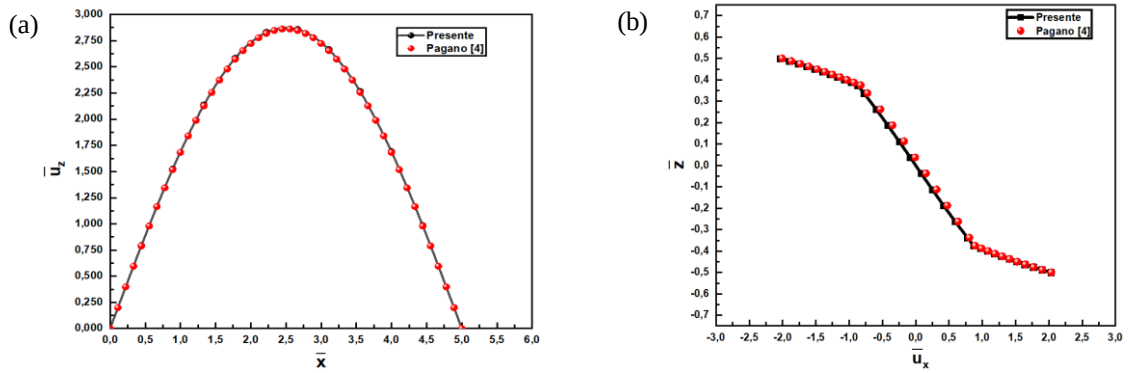


Figure 3. (a) shows the deflection at $z = 0$, and (b) shows axial displacement at $x = 0$.

Figures 4 and 5 illustrate the variation of shear and normal stresses across entire beam domain, in contrast to the localized cross-sectional views shown in Figs. 2-a and 3-b. Figures 4-a and 4-b present the shear stress field obtained from the reference solution (Pagano [4]) and the proposed model, respectively. Similarly, Figs. 5-a and 5-b show the normal stress field for the reference solution and the proposed model. Figure 4 demonstrated excellent agreement between the reference and proposed results throughout the beam domain, while also highlighting the continuity of the shear stress field as predicted by the constitutive model. In Fig. 5, very good agreement is also observed between the proposed model and the reference solution for the normal stress distribution.

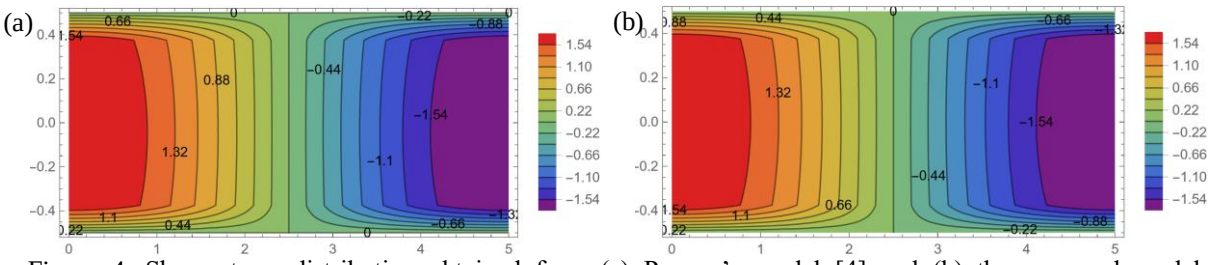


Figure 4. Shear stress distribution obtained from (a) Pagano's model [4] and (b) the proposed model. Quantitative agreement: WAPE = 0.73%.

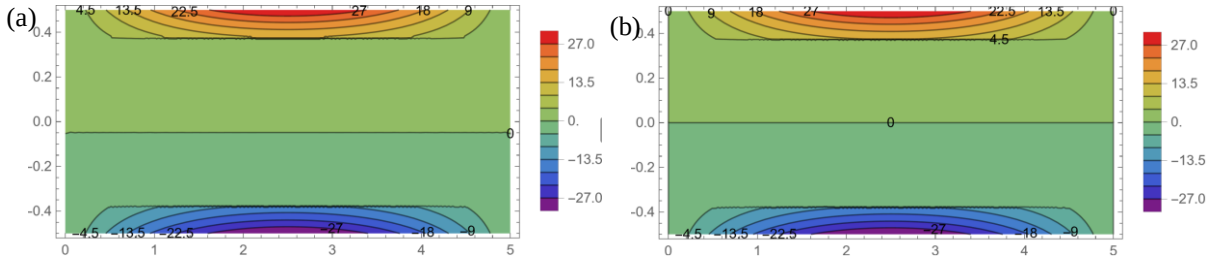


Figure 5. Normal stress distribution obtained from (a) Pagano's model [4] and (b) the proposed model.

Figures 6 and 7 illustrate the variation of deflection and longitudinal displacement across the entire beam domain. Figures 6-a and 6-b present the reference solution (Pagano [4]) and the proposed model for deflection, respectively. Similarly, Figs. 7-a and 7-b show the longitudinal displacement field for Pagano [4] and for the proposed model. As shown in Fig. 6, there is a good agreement between the proposed model and the reference models, with a slight discrepancy observed in the central region of the beam. This difference can be attributed to the absence of transverse normal strain in the proposed model, i.e., the lack of the quasi-3D effects. Fig. 7 also demonstrated strong agreement between the proposed model and the reference.

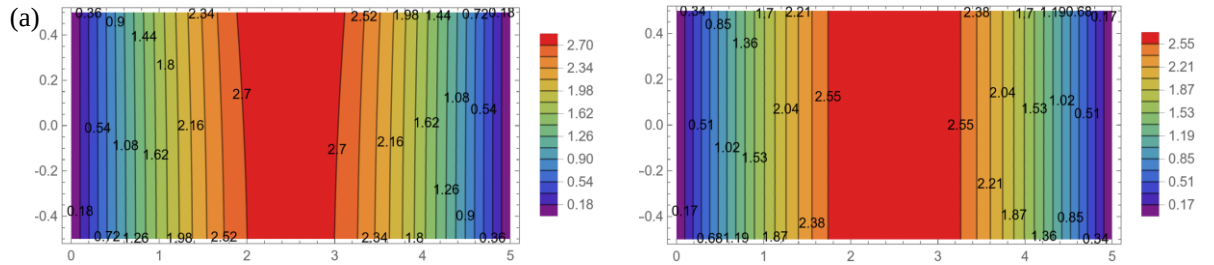


Figure 6. Deflection obtained from (a) Pagano's model [4] and (b) the proposed model. Quantitative agreement: WAPE = 0.36%.

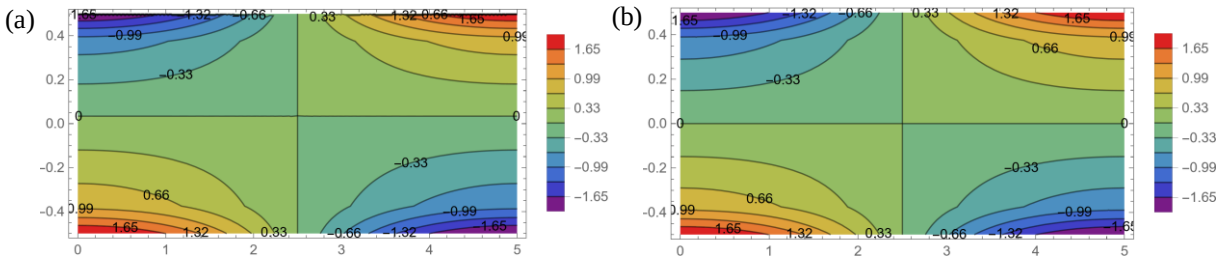


Figure 7. Longitudinal displacement obtained from (a) Pagano's model [4] and (b) the proposed model.

3 Conclusions

This work proposed a new kinematic formulation for the static flexural analysis of fiber-reinforced laminated composite beams, accounting for the continuity of shear stresses at the layer interfaces. The governing equations were derived using the Lagrange Principle, and Rayleigh-Ritz method was employed for the numerical solution.

To validate the proposed formulation, transverse and longitudinal displacements, as well as shear and normal stresses, were compared with the reference results of Pagano [4] for a simply supported cross-ply beam subjected to sinusoidal loading. The Weighted Absolute Percentage Error (WAPE) metric was used for this comparison, and the resulting indicated excellent agreement.

By enforcing interlaminar shear-stress continuity through kinematic compatibility, the proposed model provides a low-cost yet accurate alternative to full 3D elasticity analyses for the design and preliminary assessment of thick fiber-reinforced sandwich beams.

Acknowledgements. T.A.M. would like to thank CAPES for the master's scholarships granted. F. C. R. tanks FAPITEC for the financial support through the Universal Project No. 019203.01702/2024-6, and FAPITEC/SE/FUNTEC - PRAPEC (Call No.05/2025).

Authorship statement. The authors hereby confirm that they are the sole liable persons responsible for the authorship of this work, and that all material that has been herein included as part of the present paper is either the property (and authorship) of the authors, or has the permission of the owners to be included here.

References

[1] Reddy JN. Mechanics of laminated composite plates and shells. 2nd ed. Boca Raton: CRC Press; 2003.
[2] Millard JR. Mechanics of composite materials. 2nd ed. Boca Raton: CRC Press; 1999.
[3] Kaw AK. Mechanics of composite laminates. 2nd ed. Boca Raton: CRC Press; 2006.
[4] Pagano NJ. Exact solutions for composite laminates in cylindrical bending. J Compos Mater. 1969;3(4):398.
[5] Tessler A, Di Sciuva M, Gherlone M. A refined zigzag beam theory for composite and sandwich beams. J Compos Mater. 2009;43(9):1051–1081.
[6] Reddy JN. Energy principles and variational methods in applied mechanics. 3rd ed. Hoboken: Wiley; 2017.
[7] Nguyen ND, Vo TP, Tran VT, et al. A Chebyshev–Ritz solution for size-dependent analysis of the porous microbeams with various boundary conditions. Int J Mech Mater Des. 2023;19(4):861–881.